Eighth Australasian Fluid Mechanics Conference, University of Newcastle, N.S.W., 28 November/2 December 1983.

ON THE ROLL OF SMALL-SCALE BREAKING WAVES IN AIR-SEA INTERACTION AND OCEANIC REMOTE SENSING

M.L. BANNER

OCEAN SCIENCES DIVISION

R.A.N. RESEARCH LABORATORY, DARLINGHURST, N.S.W. 2010 AUSTRALIA

SUMMARY Remote sensing techniques for determining ocean wave spectra and windstress by active microwave satellite-based instruments depend directly on microwave backscattering from the ocean surface microstructure. The results described here relate to dynamical aspects of small-scale breaking waves and to their possible role in microwave backscattering.

1. INTRODUCTION

The capability of active microwave instruments to remotely sense the dominant ocean waves and the wind-stress from satellites has been demonstrated by Sea Sat which flew in 1978. These active microwave remote sensing techniques offer 24 hour, all-weather operating capability. Coherent microwaves beamed from the satellite are backscattered as a result of their interaction with the centimetric wavelength components of the ocean wave spectrum. The primary scattering mechanism is believed to be Bragg resonant backscatter. This has been established in a series of laboratory investigations by the U.S. Naval Research Laboratory (see for example Wright (1978)). The strong dependence of the ocean surface microstructure on the local windstress and on straining by underlying swell leads to local modulations of the backscattered microwave power which are then interpreted in terms of the oceanic variable of interest.

A recent ocean microwave experiment from an offshore oil platform (Wright et al (1980)) reported inexplicably high backscattered power modulations. The model which accounted so well for the laboratory results (Keller and Wright (1975)) was found to underpredict the observed oceanic microwave modulation levels by a wide margin. The conclusion of Wright et al (1980) was that the modulation of the microwave return, interpreted as being proportional to the modulation of local Bragg resonant waves, was largely due to a source substantially stronger than the straining, tilting and variations of the Bragg resonant waves due to the orbital motions of the underlying swell. They suggest the possible importance of modulation of the windstress over the swell. With short wave growth rates known to be proportional to the windstress, this could be an important factor. However, no direct data on modulated windstress is presently available. It is possible that the local augmentation of windstress associated with the separated air flow over breaking waves (Banner and Melville (1976)) provides a basis for modulated windstress if the small-scale breaking waves were distributed differentially over the swell, as appears to be the case from casual observation.

In the present contribution some recent results which pertain to the dynamics of short wind-waves are described, in particular the modification to the atmospheric input to a short gravity wave component after the onset of breaking of that component. An evaluation of the strength of this effect is given. Also discussed are some initial results of a study aimed at examining the possible significance of small-scale breaking waves as direct contributors to microwave backscattering. This has revealed some interesting new properties of breaking zones and their microwave reflectivity characteristics. A preliminary assessment of these findings is given in section 4.

2. EXPERIMENTAL CONFIGURATION

The results reported here were obtained in a small wind-wave tank, configured as shown in figure 1.

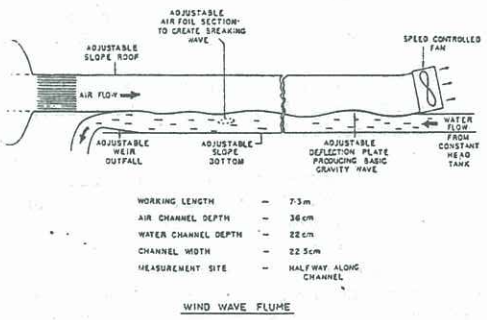

Figure 1. Experimental wind-wave flume configuration

This enabled the probing of a stationary wave field. Using an airfoil-section subsurface obstacle, a steady breaking wave or very steep unbroken wave could be generated at the measurement site. The axial flow fan drew air over the wave system at a constant rate. The following measurements were carried out using the techniques indicated in each section.

2.1 Surface Pressure Distributions Over Breaking and Unbroken Short Gravity Waves

The combination of a compact (10 mm dia.) contoured disk sensor and kiel tube (shielded total tube) (3.175 mm outside dia.) was used in conjunction with a high resolution Barocel differential electronic manometer to measure the variation of static pressure immediately above the surface profiles of the (stationary) breaking and unbroken waves in the wind wave flume. This choice of sensors was guided by the presence of separated air flow in the lee of the breaking wave. The response of the disk was

$$p_d = p_s - \alpha \tfrac{1}{2} \rho_a U^2$$

where p_d = static pressure as sensed by the disk

p_s = true static pressure

U = mean velocity

ρ_a = air density

α = disk coefficient.

The measured dependence of α on U was determined for $0 < U < 5$ m.sec^{-1} to be $0.112 \pm .007$. A comparison test against a standard N.P.L. 1.3 mm elliptic-nosed (pitot-) static tube along a contour with low streamline curvature above a stationary breaking wave showed a close correspondence in the measured distributions of static pressure. The phase of the pressure distributions were virtually coincident while the disk-kiel combination yielded a slightly higher peak pressure magnitude, within ten percent of the static tube value.

Using the disk-kiel combination, the static pressure distributions along the breaking and non-breaking waves were measured, keeping the windspeed fixed at 4 m.sec^{-1} and the water speed fixed at - 0.8 m.sec^{-1}. This study has been extended to other windspeeds but the results are not yet available. Concurrently, the mean wave profile was determined generally using a mechanical height gauge. In the fluctuating breaking zone region and its wake, the local average wave height was determined by using an auxiliary electronic contact circuit operating through the height gauge. A 50% intermittency criterion gave the mean height. The pressure and wave profile data enabled calculation of the wave-coherent momentum flux $< p \frac{\partial \eta}{\partial x} >$ due to the pressure. In this expression, p is the local surface pressure, $\frac{\partial \eta}{\partial x}$ is the local surface slope in the direction aligned with the wave vector (x-direction) and < > denotes the spatial average along the x-direction over a wavelength.

2.2 Local Microwave Scattering Properties of Small-Scale Breaking Waves (with E.H. Fooks, Electrical Engineering, U.N.S.W.)

In an extensive series of papers and reports, investigators at the U.S. Naval Research Laboratory have demonstrated the utility of the parabolic microwave antenna as a wavenumber probe. (See Wright (1978) for a survey of this technique.) In an earlier, comprehensive study by Wright et al (1972), several types of scattering wave systems associated with wind-waves at short fetch were identified on the basis of their doppler signatures. With large depression (small incidence) angles, the dominant wind-wave was the main scatterer. This was also found to be the case for lower depression angles at high wind speeds. Otherwise, the dominant scatterers were generally found to travel at the free Bragg water wave speed, augmented by wind drift effects. The authors comment that for the higher winds, the bound (scattering) waves are "perhaps not waves in the visual sense at all, but rather the broken water ahead of the crests of the dominant waves".

The wave flume described above was used for an initial investigation of the microwave scattering properties of a 0.2 m wavelength breaking wave. This scale was selected as it is characterized by negligible observable air bubble entrainment in the breaking zone. The X-band (9 GHz, 3.2 cm wavelength) microwave transmitter-crystal (square-law) detector system operating through a pyramidal horn was used to measure the backscattered power. To localize the illumination area and provide an approximately plane coherent wave front for the microwaves, an aperture of adjustable width was used just above the wave. The aperture was made from microwave absorbing sheet and was traversed in conjunction with the microwave apparatus to obtain the local reflectivity of different sections of the breaking wave profile. For the results reported here, the depression angle was 50° and the polarization was vertical. The throat of the horn was at a distance of 0.60 m from the water surface measured along the axis of the microwave device. A T.S.I. Model 1076 Averaging DVM was used to determine the mean backscattered power levels. For analysis of the temporal variability of the return power, a HP Model 3582 A Spectrum Analyzer was used. This device was also used in conjunction with two closely matched wave height-capacitance gauges (wire dia. ~ 0.1 mm) with a gain of 10 mm/volt to determine the temporal variability and dispersion characteristics of the hydrodynamic disturbances associated with the breaking zone.

3. RESULTS

3.1 Surface Pressure Distributions Over Breaking and Unbroken Short Gravity Waves

The surface pressure distributions over a breaking and moderately steep unbroken wave for the same free stream wind speed of 4 m.sec^{-1} are shown in figure 2 and figure 3 respectively. They are notably different in character, particularly with regard to the position of the pressure peak with respect to the slope of the underlying wave profile. It is this relative phasing which determines the wave-coherent momentum flux due to the air pressure distribution. For the breaking wave, the pressure peak leads the breaking crest by about 240°. For the unbroken wave, this angle barely exceeds the potential flow value of 180°.

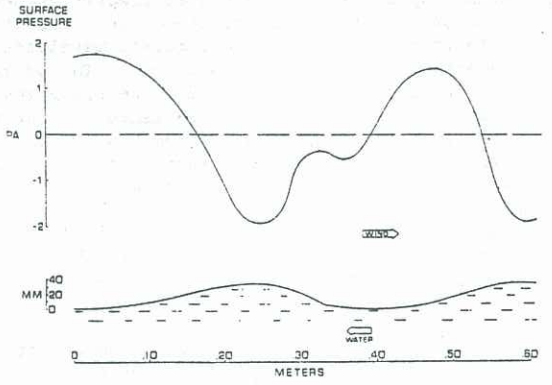

Figure 2. Surface pressure distribution over breaking wave. Windspeed = 4 m.sec^{-1}

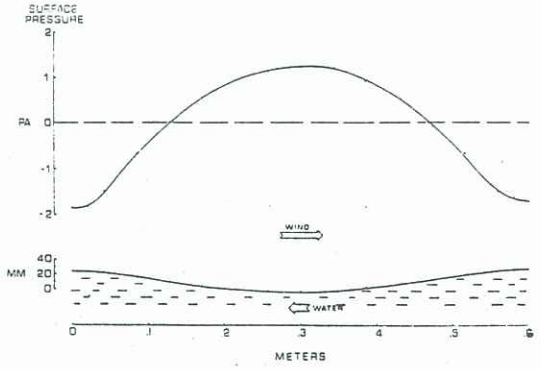

Figure 3. Surface pressure distribution over unbroken wave. Windspeed = 4 m.sec^{-1}

For the windspeed reported here, the data shown in figures 2 and 3 implies a wave-coherent momentum flux i.e. a momentum flux to the wave field which is enhanced by a factor of about 20 due to the breaking wave. (The total momentum flux (i.e. windstress) is enhanced locally in similar proportions according to

Banner and Melville (1976).)

These results can be used to estimate the strength of the augmented input to the wave field at breaking due to pressure forces. Firstly, using typical wave tank estimates of the windstress for this wind speed (see Plant and Wright (1977)), the local augmentation of input $< p \frac{\partial \eta}{\partial x} >$ to the wave field at breaking is of the same magnitude as the mean windstress, i.e.

$$\frac{< p \frac{\partial \eta}{\partial x} >}{\rho_a U_*^2} \sim O(1) \qquad 3.1(a)$$

where U_* = wind friction velocity. Secondly, an equivalent 'growth rate' can be defined as the ratio of the horizontal momentum added per wave period to the momentum density of the breaking wave (including the spilling zone contribution). The present results lead to an equivalent growth rate β given by

$$\beta = \frac{< p \frac{\partial \eta}{\partial x} >}{M_{TOT}} \sim 0.13 \left[\frac{U_*}{c}\right]^2 f \qquad 3.1(b)$$

Here M_{TOT} = momentum density of breaking wave and its spilling zone
f = wave frequency
c = wave phase speed

The significance of these findings is discussed in section 4.

3.2 Local Microwave Scattering Properties of Small-Scale Breaking Waves

Distributions of backscattered mean microwave power over 20 cm breaking and steep unbroken waves measured with a 10 cm aperture length are shown in relation to their wave profiles in figure 4 and figure 5 respectively. Despite the relatively narrow aperture of 10 cm, the relative reflectivity at X-band with vertical polarization of the breaking wave

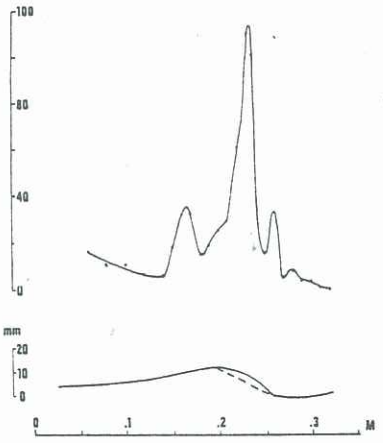

Figure 4. Distribution of backscattered microwave power in relation to breaking wave profile (arbitrary, linear vertical scale)

is substantial. Also apparent is a fairly strong localization of the peak return just ahead of the breaking wave crest, a feature which was unaltered by small variations (± 10 mm) of the aperture length.

The fluctuating instantaneous microwave return power signal appeared to be characterized by a dominant frequency in the 10 - 15 Hz range. This motivated an investigation into the hydrodynamic disturbances in

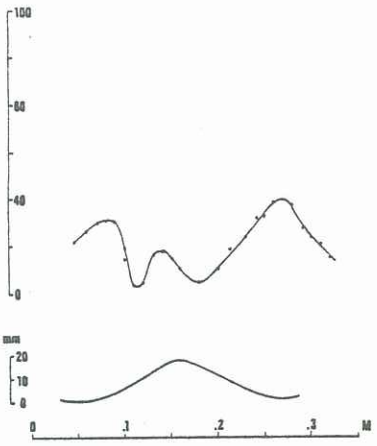

Figure 5. Distribution of backscattered microwave power in relation to unbroken, steep wave profile (same vertical scale as in figure 4)

the breaking zone. Frequency spectra from a wave height gauge also showed a similar dominant peak in this frequency range. The peak frequency was found to have a weak dependence on the probe position in the breaking zone and on the degree of breaking. From these sources, variations of about ± 2 Hz around a mean frequency of about 12.5 Hz were observed. Figure 6 shows the close correspondence between the two effects. The proximity of the two spectral

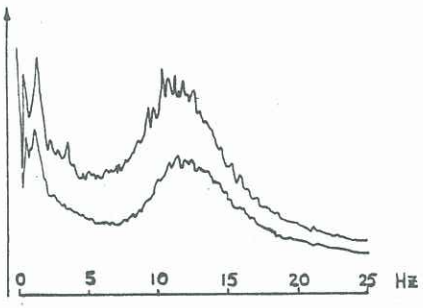

Figure 6. Frequency spectra of hydrodynamic surface disturbances (upper curve) and microwave return power (lower curve) in the breaking zone just ahead of the crest (arbitrary, linear vertical scale)

responses was typical of the cases examined with different degrees of breaking intensity. In view of the square-law crystal detector used for the microwave return, this result ruled out the possibility of standing wave modes of specular scatter as the dominant microwave return would then have been at twice the dominant disturbance frequency. Indeed, phase-coherency measurements using two wave probes showed the presence of a range of coherent length scales in the wave vector direction. An example is shown in figure 7 for the 14.4 Hz frequency component. Here the presence of travelling wave modes with wavelengths embracing the Bragg wavelength ($0.5 \lambda_m \sin \theta_d$, where λ_m = microwavelength = 3.2 cm, θ_d = depression angle) is apparent, despite the local distortion by the underlying steep, short gravity wave. The longitudinal coherence was found to persist over

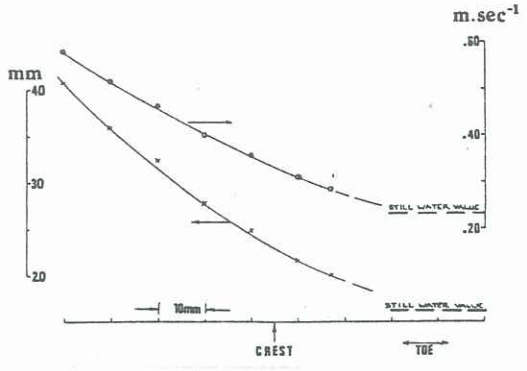

Figure 7. Dispersion characteristics for 14.4 Hz frequency component. Left hand curve is the disturbance wavelength, right hand curve is its phase velocity backwards relative to the stationary breaking wave

at least the wavelength of the underlying breaking wave. The lateral coherency (parallel to the breaking crest) was found to be much less extensive, being of the order of the Bragg wavelength (~ 20 mm).

4. DISCUSSION

The wave-coherent momentum flux results demonstrate a significantly enhanced dynamical coupling between the wind and wave field at breaking events. Local phase shifts of around 240° between the air pressure and wave height were observed to be induced by the stationary breaking wave in this study. This is comparable with the values of around 225° - 250° reported for propagating breaking wind-waves in a wave tank by Wu, Hsu and Street (1977). The source of this effect is the air flow separation known to occur ahead of the crests of breaking waves (Banner and Melville (1976)).

These findings are important in the context of modelling the evolution of a short wave spectrum which is invariably characterized by saturation and breaking of the dominant wave component. It appears that the form of the atmospheric input source function which applies to an unsaturated wave compoment over a wide range of $\left[\frac{U_*}{c}\right]$ conditions is still applicable when the wave component is breaking. No doubt much of the added momentum flux at breaking serves to sustain the breaking and concomitantly augment the local wind-stress. It also appears that with the estimated quadratic dependence on $\left[\frac{U_*}{c}\right]$, the strength of this effect diminishes rapidly with wavelength. However, for the short gravity wind-wave spectrum, it is of primary importance in the dynamics.

The initial probing of the microwave reflectivity of small-scale breaking gravity waves has revealed an interesting new property of breaking zones. The stationary breaking zones of short (~ 20 cm wavelength) gravity waves investigated here produced hydrodynamic travelling-wave disturbances in the centimetric wavelength range. Depending on the microwavelength and depression angle, these disturbances can contribute to the resonant Bragg wave spectral component. The complementary microwave measurements reported here are consistent with an enhanced local return from this class of disturbance.

From the extensive measurements by the N.R.L. group (Wright et al (1972)) on microwave reflectivity of wind-waves over a wide range of wind speeds, fetches and look angles, it seems that this mechanism will be a contributor to the resonant wave doppler spectrum. Though it appears that free waves in the system are often the dominant contributor to the doppler spectrum, the case of dominant scatterers travelling near the dominant wave speed rather than the free Bragg wave speed is also reported for some depression angles and wind speeds. In any event, this initial study has identified breaking zones as belonging to the class of hydrodynamic structures which are sources of microwave backscatter in the remote sensing of ocean waves and windstress. A more extensive study of this effect certainly appears to be warranted and is currently in progress.

5. REFERENCES

BANNER, M.L. and MELVILLE, W.K. (1976) On the separation of air flow over water waves. J. Fluid Mech., 77, 825-42.

KELLER, W.C. and WRIGHT, J.W. (1975) Microwave scattering and the straining of wind-generated waves. Radio Science, 10, 2, 139-147.

PLANT, W.J. and WRIGHT, J.W. (1977) Growth and equilibrium of short gravity waves in a wind-wave tank. J. Fluid Mech, 82, 767-783.

WRIGHT, J.W., PLANT, W.J. KELLER, W.C. and JONES, W.L. (1980) Ocean wave-radar modulation transfer functions from the West Coast Experiment. J. Geo. Res. 85, C9, 4957-4966.

WRIGHT, J.W. (1978) Detection of ocean waves by microwave radar; the modulation of short gravity-capillary waves. Boundary Layer Meteorology, 13, 87-105.

WRIGHT,, J.W., DUNCAN, J.R. and KELLER, W.C. (1972) Wind-wave studies. Part 1, Doppler Spectra. US Naval Research Laboratory Report 7473. Washington DC, 20 pp.

WU, H.Y., HSU, E.Y. and STREET, R.L. (1977) The energy transfer due to air input, non-linear wave-wave interaction and whitecap dissipation associated with wind-generated waves. Tech. Rept. 207 Dept. of Civil Eng., Stanford Univ., 158 pp.